INTERNATIONAL ATOMIC ENERGY AGENCY
UNITED NATIONS EDUCATIONAL, SCIENTIFIC AND CULTURAL ORGANIZATION

INTERNATIONAL CENTRE FOR THEORETICAL PHYSICS
34100 TRIESTE (ITALY) - P.O.B. 586 - MIRAMARE - STRADA COSTIERA 11 - TELEPHONE: 2240-1
CABLE: CENTRATOM - TELEX 460392-1

H4.SMR/285 - 8

WINTER COLLEGE ON
LASER PHYSICS: SEMICONDUCTOR LASERS
AND INTEGRATED OPTICS

(22 February - 11 March 1988)

LIGHT-MATTER INTERACTION IN SEMICONDUCTORS

H. Melchior
Swiss Federal Institute of Technology
Zürich, Switzerland

BASIC CONFIGURATION OF LIGHTWAVE SYSTEMS

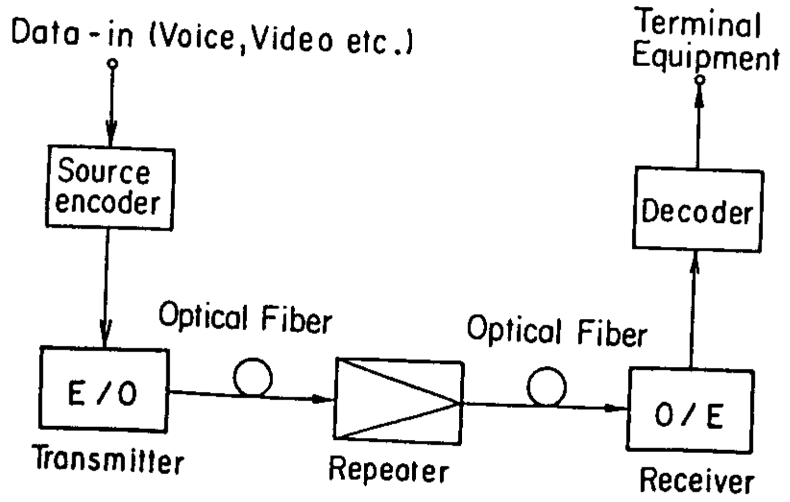

- OVERVIEW OVER LIGHT TRANSMISSION AND INTERACTION-EFFECTS WITH MATTER

- LIGHT GENERATION AND ABSORPTION

  EINSTEIN'S THEORY OF PLANCK'S BLACKBODY RADIATION

  SPONTANEOUS AND STIMULATED EMISSION IN SEMICONDUCTORS

  GAIN IN SEMICONDUCTOR LASERS

  BASIC PHOTODETECTION EFFECTS IN PHOTODETECTORS

- PHYSICAL EFFECTS LEADING TO MODULATION OF LIGHT

HIGH-SPEED LIGHTWAVE TRANSMISSION SYSTEM

TERRESTRIAL AND UNDERSEA SYSTEMS

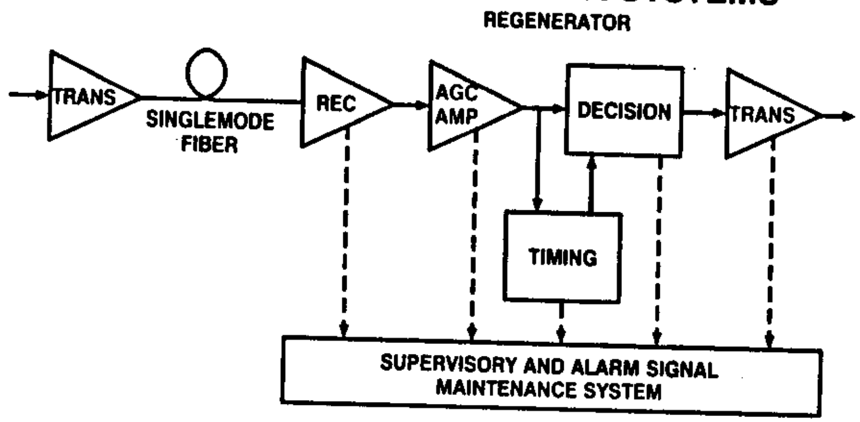

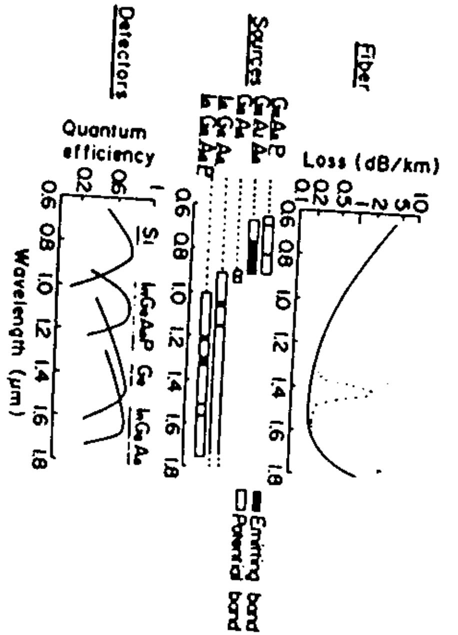

OPTICAL COMMUNICATION SYSTEMS

Optical Fiber

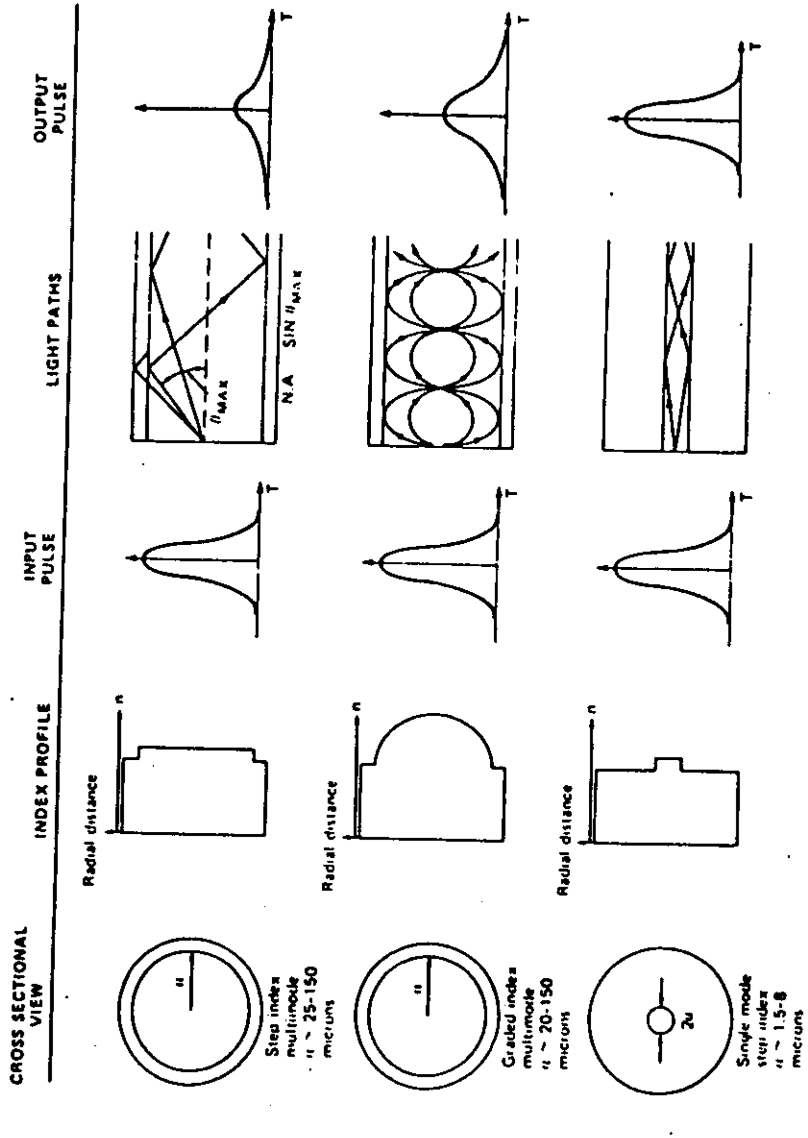

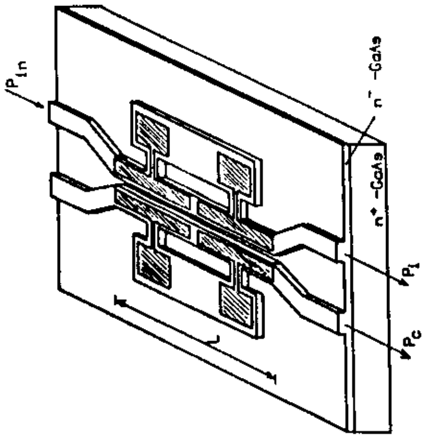

GaAs STEPPED ΔB DIRECTIONAL COUPLER

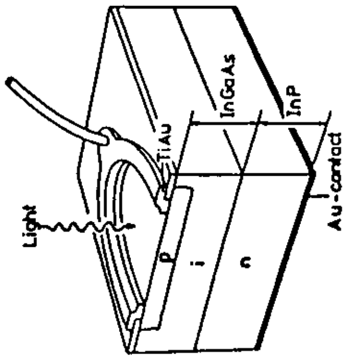

InGaAs p-i-n Photodiode for 1 - 1.6 μm

SEMICONDUCTOR LASER

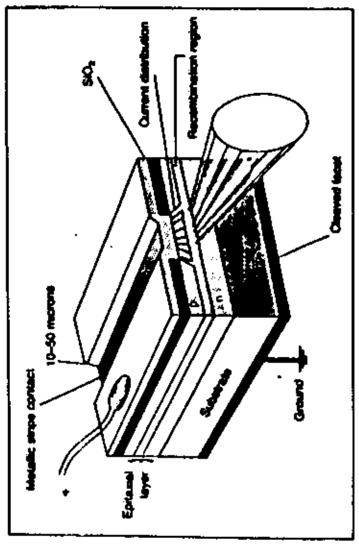

LIGHT TRANSMISSION AND INTERACTION WITH MATTER

LIGHT GENERATION	LIGHT TRANSMISSION	LIGHT ABSORPTION
"Particle Nature of Light"	"Wave Nature of Light"	"Particle Nature of Light"
Excited carriers generate photons	Electromagnetic waves decribed by Maxwell's equations	Absorbed photons excite electron–hole–pairs
Quantum Mechanical Effect	Electromagnetic waves interact with lattice atoms and electrons ⇓ Polarization of Matter	Quantum Mechanical Effect

Maxwell Equations

$\mathrm{rot}\, E = -\frac{\partial B}{\partial t}$; $\mathrm{rot}\, H = j + \frac{\partial D}{\partial t}$

$\mathrm{div}\, D = \rho$; $\mathrm{div}\, B = 0$

Optics: $j = 0$; $\rho = 0$

+ isotropic nonmagnetic material with linear, dispersion-free, hysteresis-free, scalar susceptibility: χ

$B = \mu_0 H$; $D = \varepsilon_0 \varepsilon_{rel} E$

$D = \varepsilon_0 E + P$; $P = \varepsilon_0 \chi E = \varepsilon_0(\varepsilon_{rel} - 1) E$

$\varepsilon_{rel} = n^2$; $c = \frac{1}{\sqrt{\mu_0 \varepsilon_0}}$

Vector Wave Equation

$\mathrm{rot}\,\mathrm{rot}\, E = -\frac{n^2}{c^2}\frac{\partial^2 E}{\partial t^2}$

if $\mathrm{div}\, E = 0$ i.e. $-E \frac{\mathrm{grad}\,\varepsilon}{\varepsilon} = 0$ one obtains the

Wave Equation

$\nabla^2 E = \frac{n^2}{c^2}\frac{\partial^2 E}{\partial t^2}$

$E \to E e^{j\omega t}$; $H \to H e^{j\omega t}$

Helmholtz Equation

$\nabla^2 E + \frac{\omega^2}{c^2} n^2 E = 0$

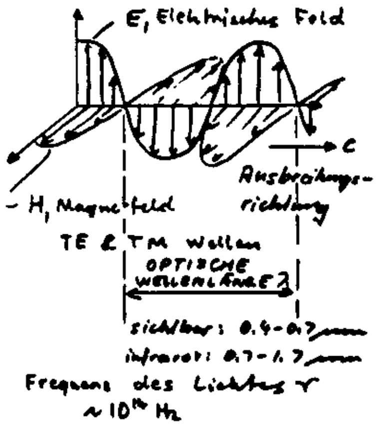

81

Basics about Energy Bands and Carrier Populations in Semiconductors

Free Electron:

Kinetic Energy $E_{kin} = \frac{m v^2}{2}$ Mass m, Velocity v

Impulse $\vec{p} = m \vec{v}$

⇓

$E_{kin} = \frac{p^2}{2m}$

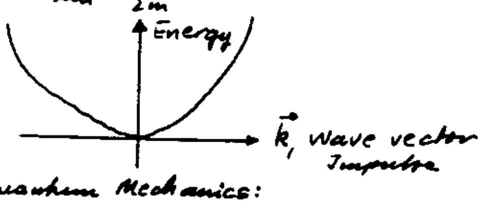

in Quantum Mechanics:

Impulse $\vec{p} = \hbar \vec{k}$

$\vec{k}$ = Wavevector

$\hbar = \frac{h}{2\pi}$; h = Plancks constant

82

Electrons in Crystals:

Electron moving in periodic potential (periodic distance a) of ideal crystal lattice:

⇒ k-values are quantized

$k_n = n \frac{\pi}{L}$ L = Length of crystal

$n = 1; 2; 3 \ldots$

up to $k = k_{max} = \frac{\pi}{a}$

⇒ Allowed energy levels for electrons split up into bands: the high density of levels separated by forbidden zones

(for $k > k_{max}$ the energy levels repeat periodically: Brillouin-zones)

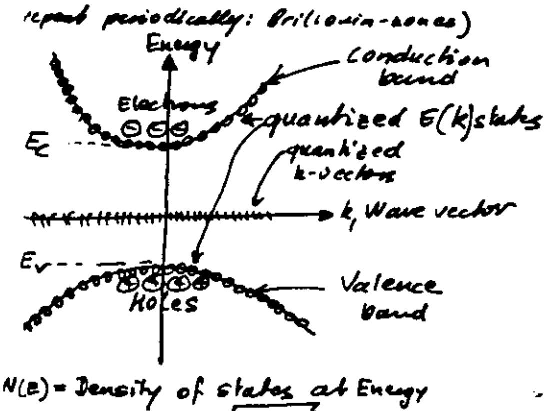

N(E) = Density of states at Energy level E ~ $\sqrt{E - E_C}$

Occupation probability of energy states:

- In thermal equilibrium the probability of occupation of an energy level E is given by the Fermi-Dirac probability distribution:

$$F(E) = \frac{1}{1+\exp\left(\frac{E-E_F}{kT}\right)} \qquad 0 \leq F(E) \leq 1$$

E_F = Fermi Level Energy

· Density of electrons in conduction band:

$$n = \int_{E_C}^{\infty} N(E)\, F(E)\, dE \Rightarrow n = N_C \exp\left(-\frac{E_C - E_F}{kT}\right)$$

- For deviations from thermal equilibrium:

$E_F \neq E_{Feq}$

$$F(E, E_{Fdyn}) = \frac{1}{1+\exp\left(\frac{E-E_{Fdyn}}{kT}\right)}$$

Carrier Concentration at Thermal Equilibrium

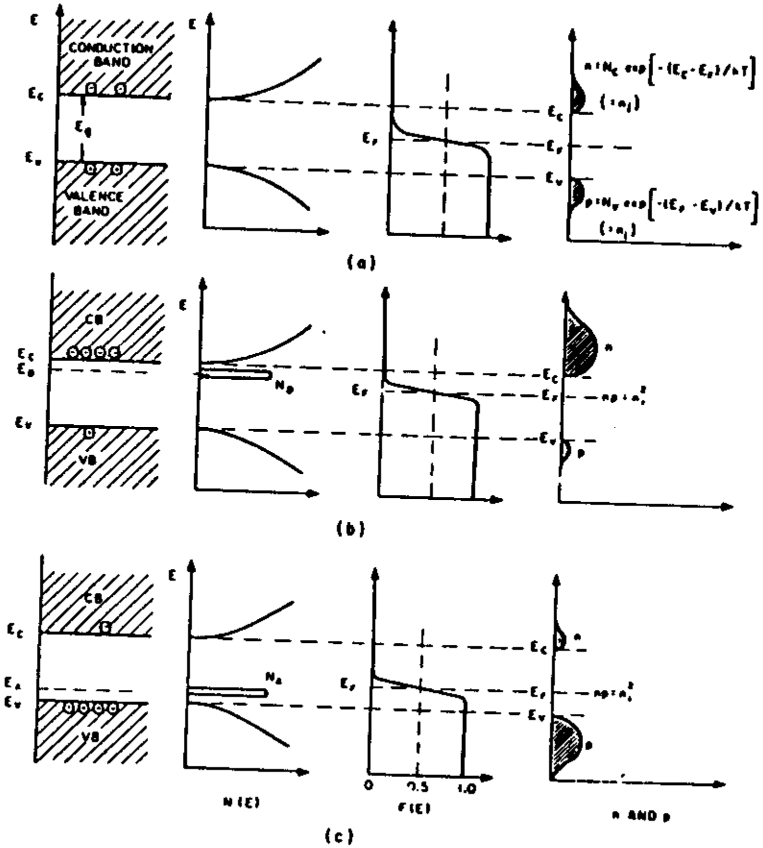

Schematic band diagram, density of states, Fermi-Dirac distribution, and the carrier concentrations for (a) intrinsic, (b) n-type, and (c) p-type semiconductors at thermal equilibrium. Note that $pn = n_i^2$ for all three cases.

Optical Absorption

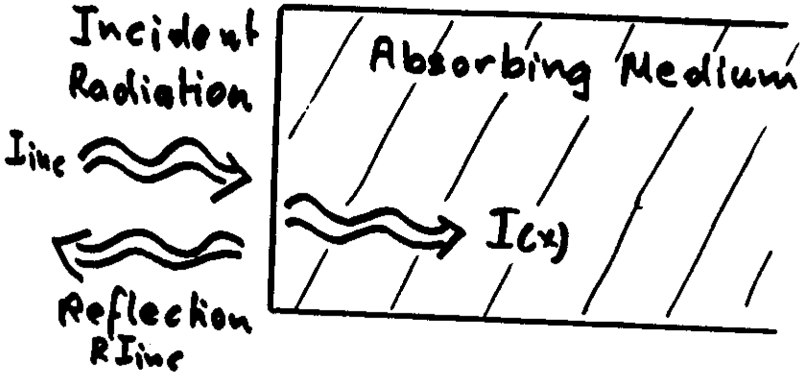

$$I_{incident}(1-R) = I(0)$$

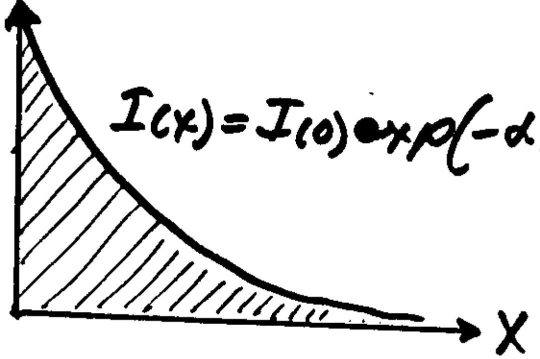

$$I(x) = I(0)\exp(-\alpha x)$$

α = Absorption Coefficient [cm^{-1}]

Light Absorbtion Coefficients

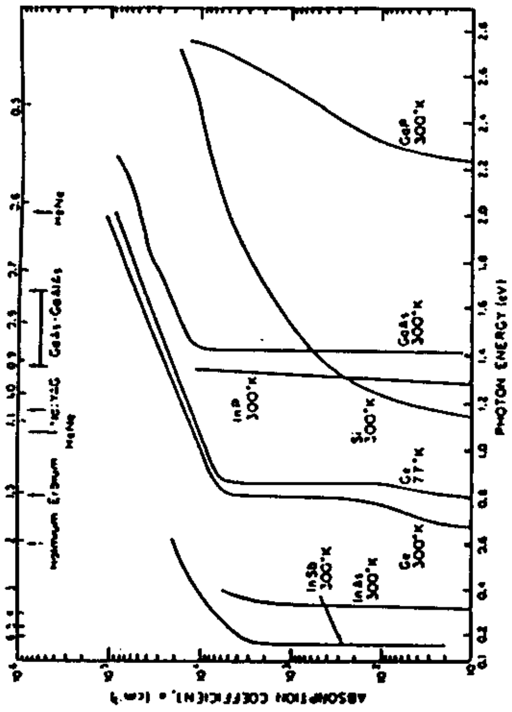

Absorption coefficients for selected semiconductors in the visible and near-infrared spectral region: InSb, InAs, Ge, Si, InP, GaAs, and GaP. Also shown are the emission energies of some promising lasers in the same spectral region.

INTERACTION OF ELECTROMAGNETIC RADIATION WITH MATTER

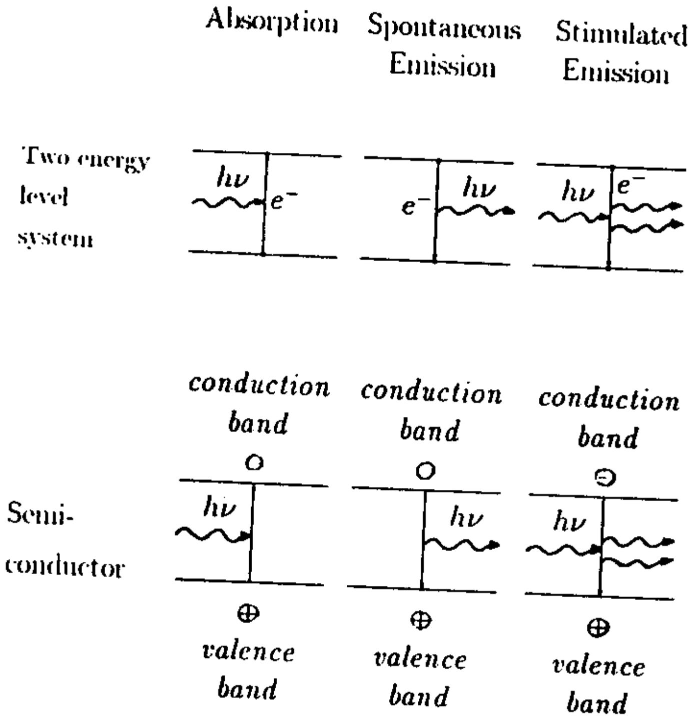

INTERACTION OF ELECTROMAGNETIC RADIATION WITH MATTER

In *ABSORPTION* a photon excites an electron to a higher energy level, thereby creating an electron–hole pair in a semiconductor.

In *SPONTANEOUS EMISSION* an electron gives up energy by moving from a higher to a lower energy level thereby creating a photon. In a direct bangap semiconductor an electron which recombines with a hole generates a photon.

In *STIMULATED EMISSION* a photon interacts with an electron and, rather than being absorbed, causes the emission of an identical photon

ENERGY BAND STRUCTURE OF DIRECT-BAND-GAP SEMICONDUCTOR

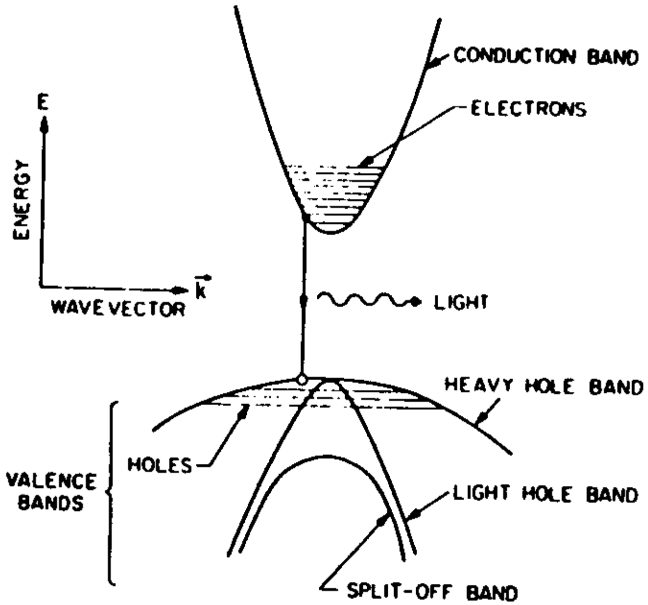

Energy versus wave-vector diagram of a direct-band-gap semiconductor showing schematically the conduction and valence bands. Three valence bands are required to model band-to-band transitions realistically. Horizontal lines show the filled energy states. Radiative recombination of electrons and holes generates photons.

ENERGY BAND STRUCTURES OF SEMICONDUCTOR WITH INDIRECT (SILICON) AND DIRECT (GALLIUM–ARSENID) BANDGAP

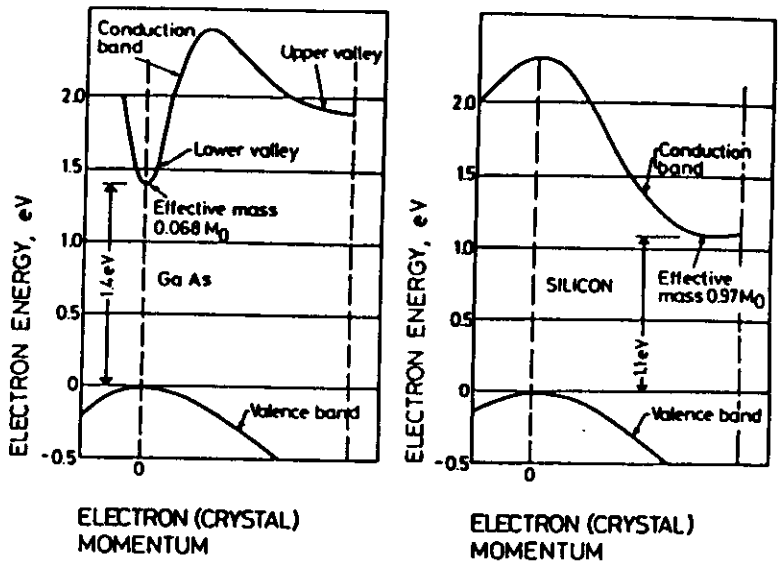

EFFICIENT LIGHT EMISSION REQUIRES SEMICONDUCTORS WITH DIRECT BANDGAP

13

BAND GAP AND LATTICE CONSTANTS OF $III-V$ COMPOUND SEMICONDUCTOR LASER AND DETECTOR MATERIALS

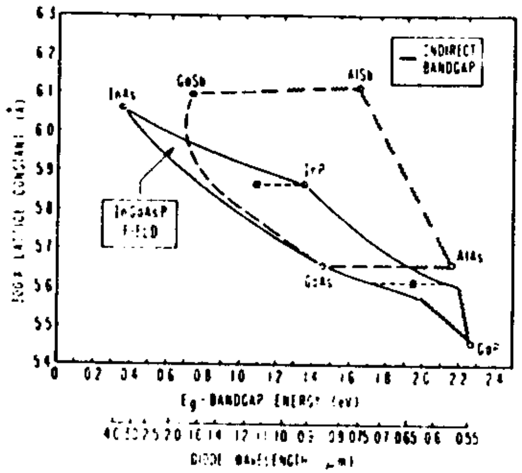

AlGaAs-GaAs Heterostructures

- Close lattice match of GaAs & AlGaAs allows epitaxial growth of AlGaAs-GaAs heterostructures with high crystal quality

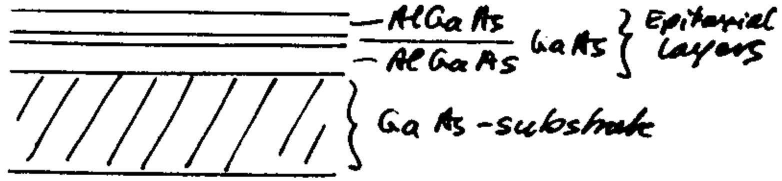

- Energy band diagram of heterostructures

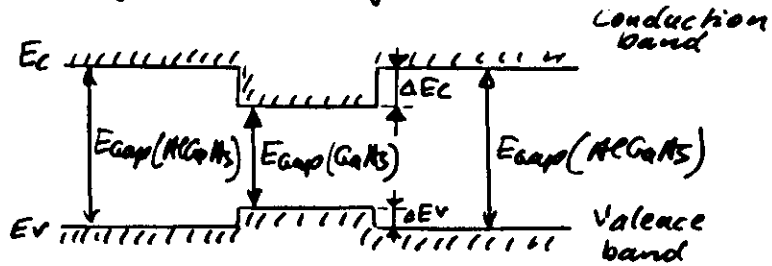

Conduction band offset:

$$\Delta E_c = 0.85\left(E_{Gap}(AlGaAs) - E_{gap}(GaAs)\right)$$

Valence band offset:

$$\Delta E_v = 0.15\left(E_{Gap}(AlGaAs) - E_{gap}(GaAs)\right)$$

PLANCK'S BLACKBODY RADIATION

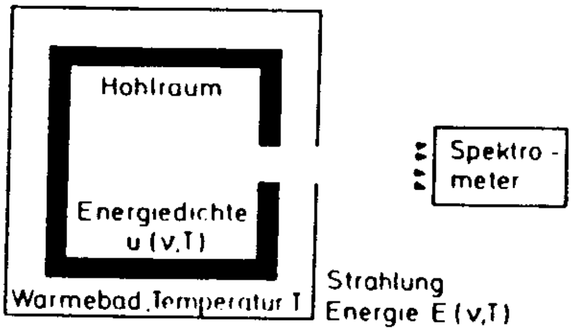

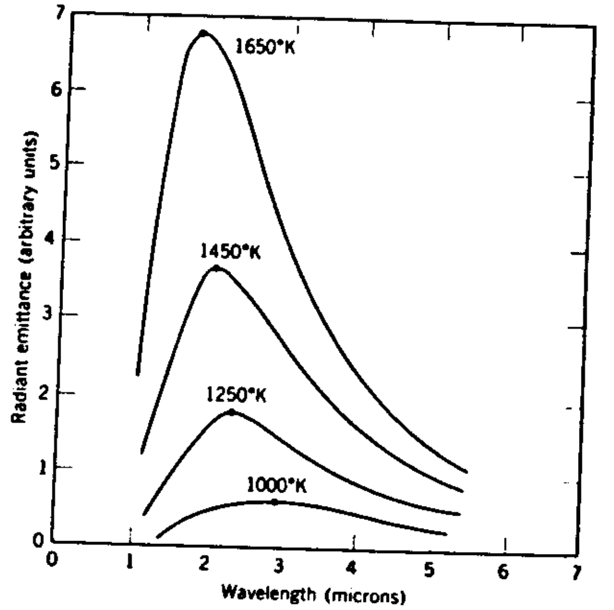

Spectral distribution of radiant power from a black body.

Spectral Energy Density:

$$u(\nu,T) = \frac{(\text{Radiation Energy in Frequency Range}) \cdot d\nu}{\text{Volume}}$$

Planck's Hypothesis:

$$u(\nu,T) = \frac{8\pi h\nu^3}{c^3}\frac{\overline{n}^3}{e^{\frac{h\nu}{kT}} - 1}$$

ν = Optical Frequency h = Planck's Constant
$h\nu$ = Photon Energy T = Temperature
c = Velocity of Light $\overline{n}$ = Refractive Index

CALCULATED DENSITY OF STATES AS A FUNCTION OF ENERGY IN CONDUCTION AND VALENCE BAND OF GALLIUM ARSENIDE

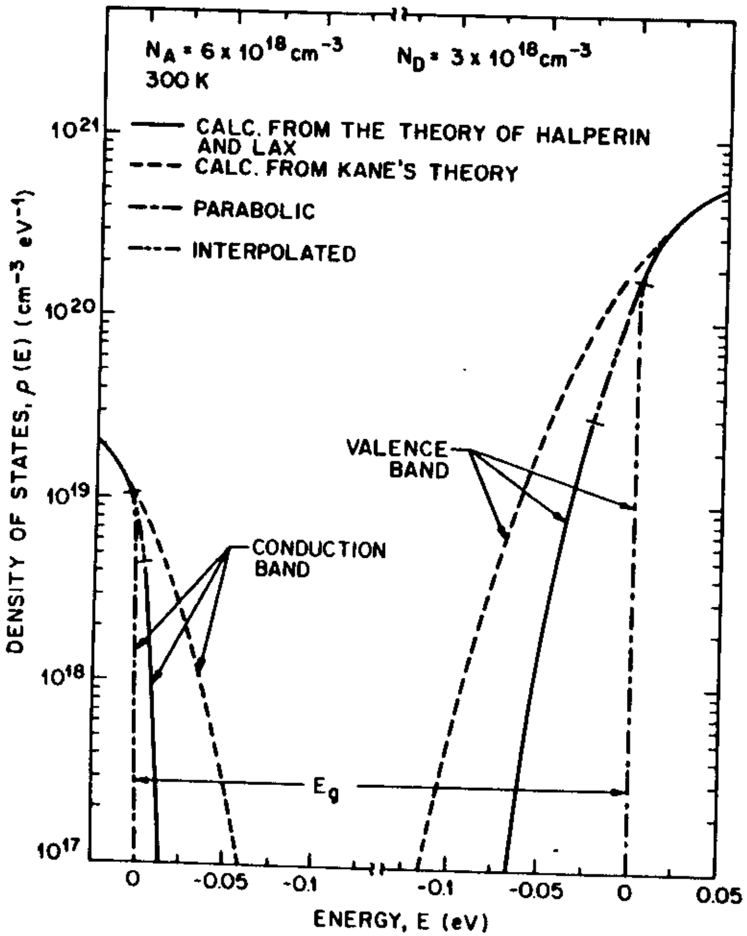

Calculated density of states versus energy in the conduction and valence bands for p-type GaAs with a net carrier concentration of 3×10^{18} cm^{-3}. The acceptor concentration $N_A = 6 \times 10^{18}$ cm^{-3}, and the donor concentration $N_D = 3 \times 10^{18}$ cm^{-3}.

ABSORPTION CURVES OF p-TYPE InGaAsP ($\lambda_{Gap} = 1.3\mu m$)

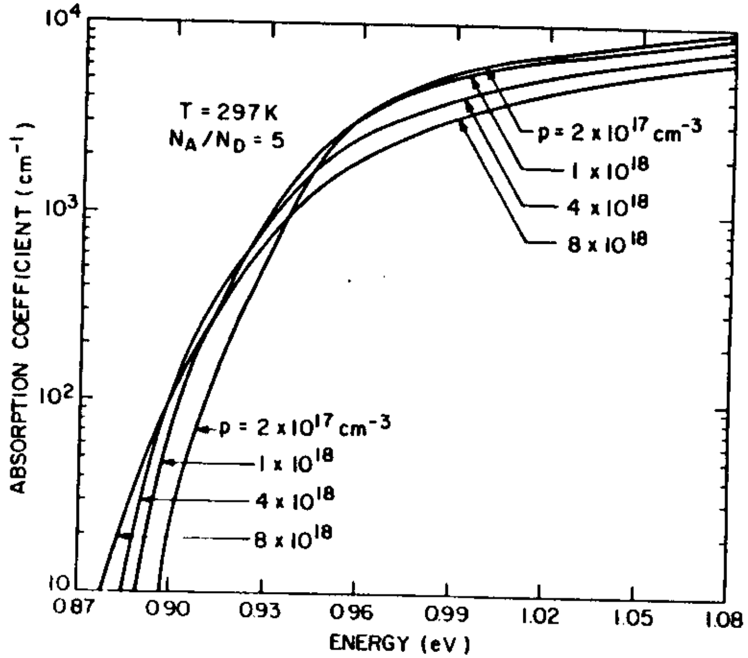

SPONTANEOUS EMISSION SPECTRA OF p-TYPE InGaAsP ($\lambda_{Gap} = 1.3\mu m$)

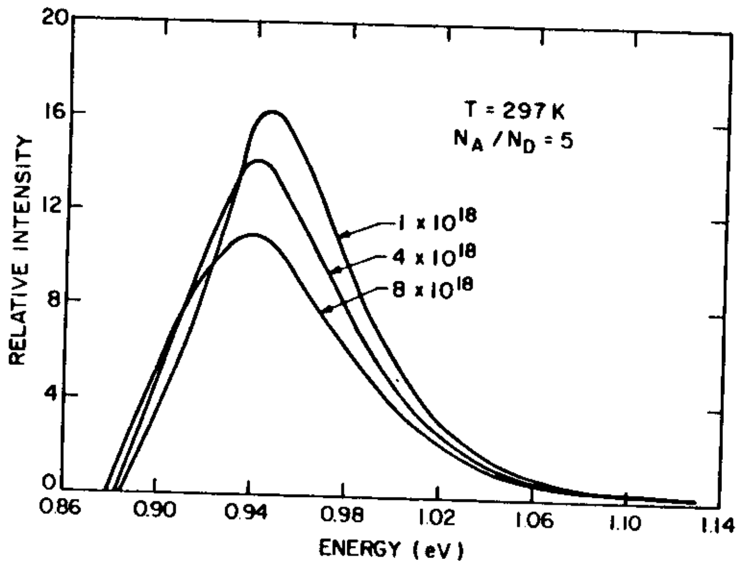

GAIN SPECTRA FOR DIFFERENT CARRIER DENSITIES IN UNDOPED InGaAsP ($E_{Gap} = 0.96eV$)

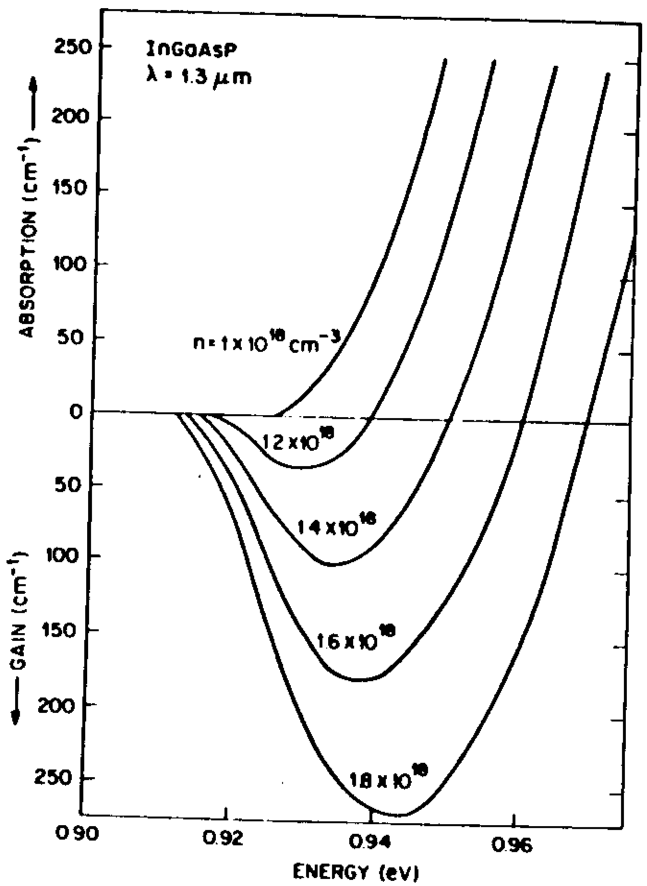

HIGHEST VALUES OF GAIN AS A FUNCTION OF INJECTED CARRIER DENSITY IN UNDOPED InGaAsP ($E_{Gap} = 0.96eV$)

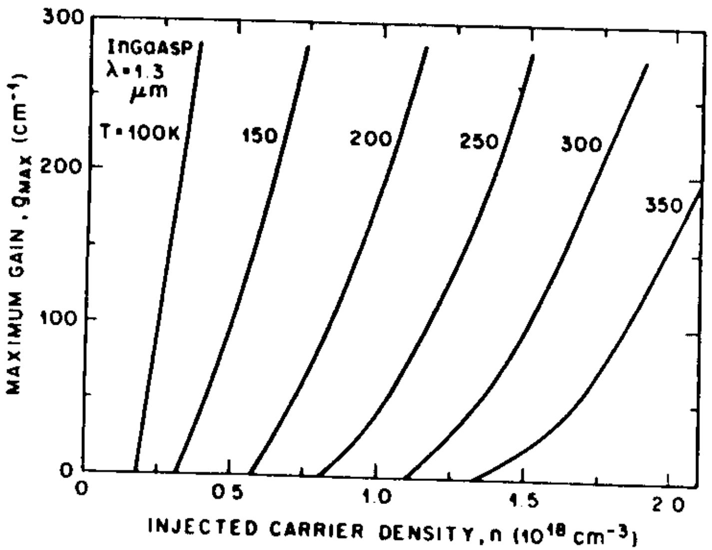

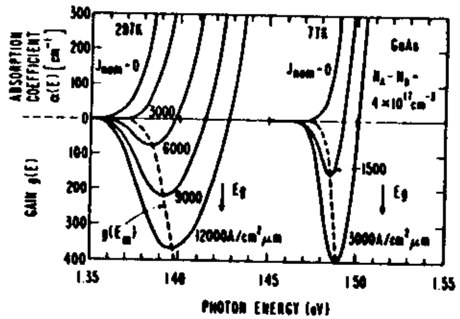

3.9 Calculated gain or absorption coefficient at 297 and 77 K as a function of photon energy for several values of the nominal current density J_{nom}. The dashed line is the photon energy at which the gain coefficient is maximum. The sample is p-type, with a net hole concentration of 4×10^{17} cm^{-3}, and it is assumed that the acceptor states have merged with the valence band

Interaction of Radiation and Atomic Systems

consider the case when the local perturbing field $E(t)$ is time harmonic so that

$$E(t) = E_0 \cos \omega t = \frac{E_0}{2}(e^{i\omega t} + e^{-i\omega t})$$

The macroscopic (oscillating) polarization is

$$P(t) = \mathrm{Re}(\varepsilon_0 \chi E_0 e^{i\omega t})$$
$$= E_0(\varepsilon_0 \chi' \cos \omega t + \varepsilon_0 \chi'' \sin \omega t)$$

where we define the atomic susceptibility by $\chi = \chi' - i\chi''$,

$$\chi''(\omega) = \frac{\mu^2 T_2 \Delta N_0}{\varepsilon_0 \hbar} \frac{1}{1+(\omega-\omega_0)^2 T_2^2 + 4\Omega^2 T_2 \tau}$$
$$\chi'(\omega) = \frac{\mu^2 T_2 \Delta N_0}{\varepsilon_0 \hbar} \frac{(\omega_0-\omega) T_2}{1+(\omega-\omega_0)^2 T_2^2 + 4\Omega^2 T_2 \tau}$$

the "precession" frequency Ω is defined by $\Omega = \mu E_0/2\hbar$.

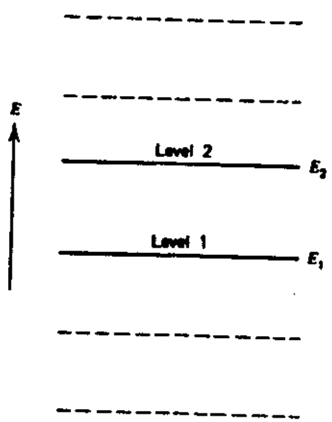

A two-level atomic system interacting with a radiation field whose frequency ω is approximately equal to $(E_2 - E_1)/\hbar$. Other nonresonant levels (shown by broken lines) are assumed to play no role in the interaction except in determining the equilibrium populations N_{2e} and N_{1e}.

relaxation time T_2

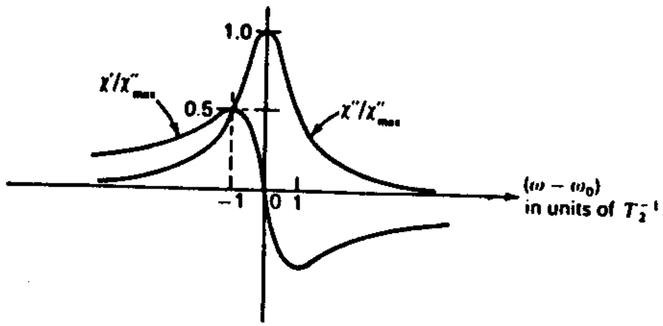

A plot of the real (χ') and imaginary (χ'') parts of the susceptibility

KRAMERS–KRONIG RELATIONS

According to a fundamental theorem of the theory of complex variables, the real and imaginary parts of a complex function $f(z)$ that has no poles in the lower (or upper) z plane are related by the Hilbert transformation (Ref. 3). When applied to the complex susceptibility function $\chi(\omega) = \chi'(\omega) - i\chi''(\omega)$, these transformations for the case of $\chi(\infty) = 0$ are

$$\chi'(\omega) = \frac{1}{\pi} \mathrm{P.V.} \int_{-\infty}^{\infty} \frac{\chi''(\omega')}{\omega' - \omega} d\omega'$$
$$\chi''(\omega) = -\frac{1}{\pi} \mathrm{P.V.} \int_{-\infty}^{\infty} \frac{\chi'(\omega')}{\omega' - \omega} d\omega' \quad (8.1\text{-}25)$$

where "P.V." stands for the Cauchy principal value of the integral that follows.

Electromagnetic Propagation in Anisotropic Media

THE DIELECTRIC TENSOR OF AN ANISOTROPIC MEDIUM

In an isotropic medium, the induced polarization is always parallel to the electric field and is related to it by a scalar factor (the susceptibility) that is independent of the direction along which the field is applied. This is no longer true in anisotropic media, except for certain particular directions. Since the crystal is made up of a regular periodic array of atoms (or molecules) with certain symmetry, we may expect that the induced polarization will depend, both in its magnitude and direction, on the direction of applied field. Instead of a simple scalar relation linking **P** and **E**, we have

$$
\begin{aligned}
P_x &= \epsilon_0(\chi_{11}E_x + \chi_{12}E_y + \chi_{13}E_z),\\
P_y &= \epsilon_0(\chi_{21}E_x + \chi_{22}E_y + \chi_{23}E_z),\\
P_z &= \epsilon_0(\chi_{31}E_x + \chi_{32}E_y + \chi_{33}E_z),
\end{aligned}
\tag{4.1-1}
$$

We can, instead of using Eq. (4.1-1), describe the dielectric response of the crystal by means of the dielectric permittivity tensor ϵ_{ij}, defined by

$$
\begin{aligned}
D_x &= \epsilon_{11}E_x + \epsilon_{12}E_y + \epsilon_{13}E_z,\\
D_y &= \epsilon_{21}E_x + \epsilon_{22}E_y + \epsilon_{23}E_z,\\
D_z &= \epsilon_{31}E_x + \epsilon_{32}E_y + \epsilon_{33}E_z.
\end{aligned}
\tag{4.1-3}
$$

From Eq. (4.1-1) and the relation

$$\mathbf{D} = \epsilon_0\mathbf{E} + \mathbf{P} \tag{4.1-4}$$

we have

$$\epsilon_{ij} = \epsilon_0(1 + \chi_{ij}). \tag{4.1-5}$$

These nine quantities $\epsilon_{11}, \epsilon_{12}, \ldots$ are constants of the medium and constitute the dielectric tensor,

assume that the medium is homogeneous, nonabsorbing, and magnetically isotropic. The energy density of the stored electric field in the anisotropic medium is

$$U_e = \tfrac{1}{2}\mathbf{E}\cdot\mathbf{D} = \tfrac{1}{2}E_i\epsilon_{ij}E_j. \tag{4.1-7}$$

THE INDEX ELLIPSOID

The surfaces of constant energy density U_e in **D** space given by Eq. (4.1-7) can be written as

$$\frac{D_x^2}{\epsilon_x} + \frac{D_y^2}{\epsilon_y} + \frac{D_x^2}{\epsilon_x} = 2U_e,$$

where ϵ_x, ϵ_y, and ϵ_z are the principal dielectric constants. If we replace $\mathbf{D}/\sqrt{2U_e}$ by **r** and define the principal indices of refraction n_x, n_y, and n_z by $n_i^2 = \epsilon_i/\epsilon_0$ $(i = x, y, z)$, the last equation can be written as

$$\frac{x^2}{n_x^2} + \frac{y^2}{n_y^2} + \frac{z^2}{n_z^2} = 1. \tag{4.3-1}$$

This is the equation of a general ellipsoid with major axes parallel to the x, y, and z directions whose respective lengths are $2n_x$, $2n_y$, $2n_z$. The ellipsoid is known as the index ellipsoid or, sometimes, as the optical indicatrix. The index ellipsoid is used mainly to find the two indices of refraction and the two corresponding directions of **D** associated with the two independent plane waves that can propagate along an arbitrary direction **s** in a crystal.

Electro-optics

in certain types of crystals, the application of an electric field results in a change in both the dimensions and orientation of the index ellipsoid. This is referred to as the electro-optic effect. The electro-optic effect affords a convenient and widely used means of controlling the phase or intensity of the optical radiation.

Since the propagation characteristics in crystals are fully described by means of the index ellipsoid (14.1-1), the effect of an electric field on the propagation is expressed most conveniently by giving the changes in the constants $1/n_x^2$, $1/n_y^2$, $1/n_z^2$ of the index ellipsoid.

Following convention (Ref. 2), we take the equation of the index ellipsoid in the presence of an electric field as

$$\left(\frac{1}{n^2}\right)_1 x^2 + \left(\frac{1}{n^2}\right)_2 y^2 + \left(\frac{1}{n^2}\right)_3 z^2 + 2\left(\frac{1}{n^2}\right)_4 yz + 2\left(\frac{1}{n^2}\right)_5 xz + 2\left(\frac{1}{n^2}\right)_6 xy = 1$$

The linear change in the coefficients

$$\left(\frac{1}{n^2}\right)_i \qquad i=1,\ldots,6$$

due to an arbitrary "low frequency" electric field $\mathbf{E}(E_x, E_y, E_z)$ is defined by

$$\Delta\left(\frac{1}{n^2}\right)_i = \sum_{j=1}^{3} r_{ij}E_j \qquad (14.1\text{-}3)$$

where in the summation over j we use the convention $1=x,\ 2=y,\ 3=z$. Equation 14.1-3 can be expressed in a matrix form as

$$\begin{vmatrix} \Delta\left(\frac{1}{n^2}\right)_1 \\ \Delta\left(\frac{1}{n^2}\right)_2 \\ \Delta\left(\frac{1}{n^2}\right)_3 \\ \Delta\left(\frac{1}{n^2}\right)_4 \\ \Delta\left(\frac{1}{n^2}\right)_5 \\ \Delta\left(\frac{1}{n^2}\right)_6 \end{vmatrix} = \begin{vmatrix} r_{11} & r_{12} & r_{13} \\ r_{21} & r_{22} & r_{23} \\ r_{31} & r_{32} & r_{33} \\ r_{41} & r_{42} & r_{43} \\ r_{51} & r_{52} & r_{53} \\ r_{61} & r_{62} & r_{63} \end{vmatrix} \begin{vmatrix} E_1 \\ E_2 \\ E_3 \end{vmatrix} \qquad (14.1\text{-}4)$$

where, using the rules for matrix multiplication, we have, for example,

$$\Delta\left(\frac{1}{n^2}\right)_6 = r_{61}E_1 + r_{62}E_2 + r_{63}E_3$$

The 6×3 matrix with elements r_{ij} is called the electrooptic tensor.

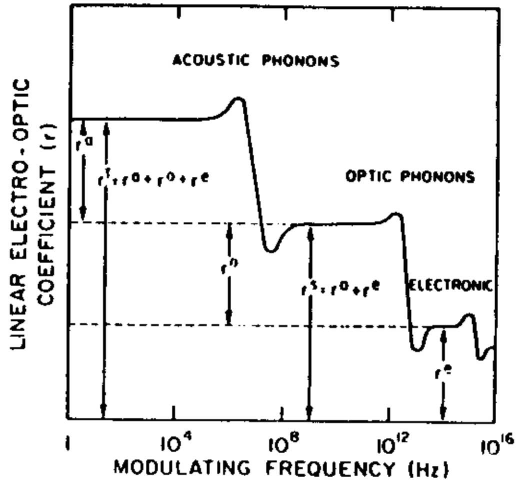

Fig. 1. Frequency dependence of the electro-optic coefficient

Guided-Wave Phase Modulator

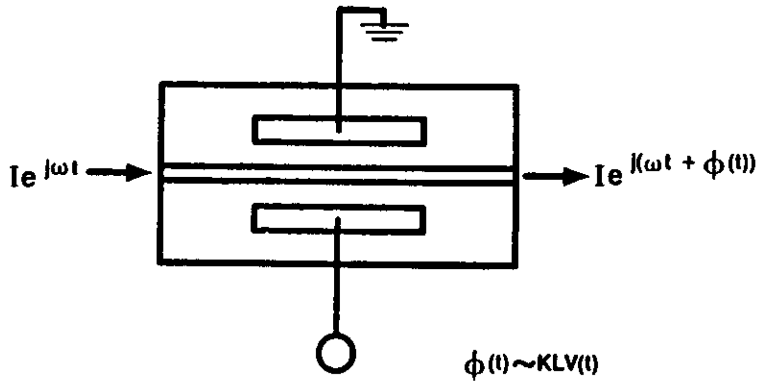

Electro-optic Devices

the electro-optic effects in crystals—the effect of an applied electric field on the propagation of electromagnetic radiation can be used to build light modulators, spectral tunable filters, electro-optic filters, beam deflectors, and so on. The use of electro-optic modulation offers the possibility of manipulating a laser beam or controlling the signal radiation at high speeds (up to the multigigahertz region), since no mechanical moving parts are involved.

ELECTRO-OPTIC LIGHT MODULATORS

The basic principle involved is that the application of the electric field changes the index ellipsoid. Consequently, the index of refraction of the crystal for the linearly polarized normal modes depends on the field strength. It is clear that the phase shift of these normal modes passing through the crystal depends on the index of refraction. After traversing a distance L in the crystal, the change in phase shift due to the applied electric field is typically

$$\Delta\phi = \frac{\pi}{\lambda} n^3 r E L,$$

where λ is the wavelength of the light, n is the index of refraction, r is the relevant electro-optic coefficient, and E is the applied electric field.

Electro-Optic Modulators Using Cubic Crystals. Cubic crystals are optically isotropic (no birefringence) and therefore offer a wide field of view in many optical systems. Here we consider the case of crystals of the $\bar{4}3m$ symmetry (zinc blende) group. Examples of this group are InAs, CuCl, GaAs, and CdTe.

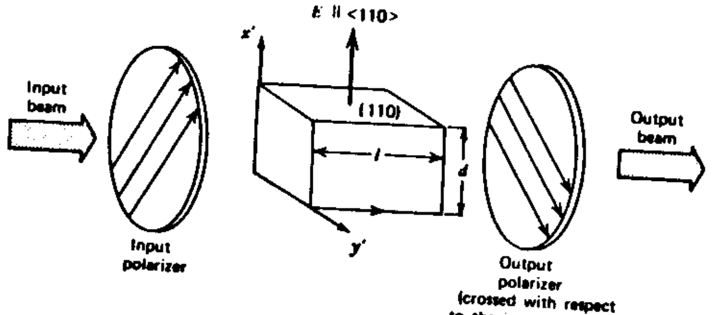

Figure 8.4. A transverse electro-optic modulator using a zinc-blende-type ($\bar{4}3m$) crystal with **E** parallel to a cube diagonal (⟨110⟩ direction).

The phase retardation is

$$\Gamma = \frac{2\pi}{\lambda} n^3 r_{41} \left(\frac{L}{d}\right) V.$$

The half-wave voltage is

$$V_\pi = \frac{d}{L} \cdot \frac{\lambda}{2n^3 r_{41}}.$$

FRANZ KELDYSH EFFECT

Electric field causes optical absorption edge to shift towards longer wavelengths

Electro-Absorption

One additional method for producing the required shift of the absorption edge to longer wavelength in a monolithic waveguide detector is electro-absorption, or the Franz-Keldysh effect. When a semiconductor diode is reverse biased, a strong electric field is established within the depletion region. This electric field causes the absorption edge to shift to longer wavelength, as shown in Fig. 15.16. Curve *A* shows the normal unbiased absorption edge for n-type GaAs with a carrier concentration of 3×10^{16} cm^{-3}. Curve *B* is a calculated Franz-Keldysh-shifted absorption edge for an applied field of 1.35×10^5 V/cm, which corresponds to 50 V reverse bias across a resulting

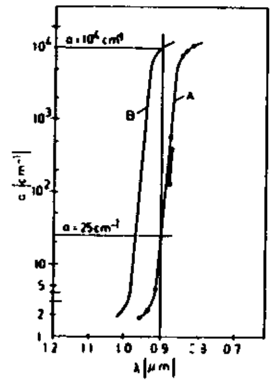

Fig. 15.16. Shift of the absorption edge of GaAs due to the Franz-Keldysh effect. (*A*) Zero-bias condition; (*B*) Reverse bias applied to produce a field of 1.35×10^5 V/cm

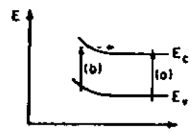

Fig. 15.17. Energy band diagram illustrating the Franz-Keldysh effect. The band bending on the n-side of a p⁺-n junction (or a Schottky barrier junction) is shown for conditions of strong reverse bias

depletion width of 3.7 μm. At a wavelength of 9000 Å this shift corresponds to an increase in α from 25 to 10^4 cm^{-1} – hardly a negligible effect!

The Franz-Keldysh effect has been well known for many years [15.21]. However it has only been applied to detector design fairly recently. The physical basis for the Franz-Keldysh effect can be understood from the simplified energy-band bending model diagrammed in Fig. 15.17. In this diagram x represents distance from the metallurgical junction plane. In the region far from the junction where there is no electric field, photons must have at least the bandgap energy $(E_c - E_v)$ to produce an electronic transition as in (a). However, within the depletion region where field is strong, a transition as in (b) can occur when a photon of less-than-bandgap energy lifts an electron partway into the conduction band, followed by tunneling of the electron through the barrier into a conduction band state. The states at the conduction band edge are, in effect, broadened into the gap so as to produce a change in effective bandgap ΔE, which is given by [15.21]

$$\Delta E = \frac{3}{2}(m^*)^{-1/3}(q h \varepsilon)^{2/3}, \qquad (15.3.1)$$

where m^* is the effective mass of the carrier, q is the magnitude of the electronic charge, and ε is the electric field strength.

The Franz-Keldysh effect greatly improves the sensitivity of a detector operating at a wavelength near its absorption edge. GaAs waveguide detectors operating at a wavelength of 1.06 μm have been demonstrated by *Nichols* et al. [15.22].

Perhaps the greatest advantage of electro-absorption detectors is that they can be electrically switched from a low absorption state to a high absorption state by merely increasing the reverse bias voltage. This makes it possible to make emitters and detectors in the same semiconductor material that are wavelength compatible. An example of a device making use of this principle is the emitter/detector terminal shown in Fig. 15.18 [15.23]. This device performs the dual function of light emitter, when forward biased, and light detector, when strongly reverse biased. Fabricated in series with a waveguide structure, as shown, it can act as a send/receive tap on an optical transmission line. Because of the large change in α produced by the Franz-Keldysh effect, operation can be very efficient. For example, consider the case of a p^+-n junction diode in n-type GaAs with carrier concentration equal to 3×10^{16} cm^{-3}, as before. Application of 50 V reverse bias changes α from 25 to 10^4 cm^{-1} at a wavelength of 9000 Å. Thus, when forward biased, the diode emits 9000 Å light into the waveguide. When reverse biased with $V_a = 50$ V, the diode need have a length of only 10^{-3} μm in order to absorb 99.9% of incident 9000 Å light. When the diode is on *standby* at zero bias, α is just 25 cm^{-1}. Hence, for a typical laser length of 200 μm, the insertion loss is only 2 dB. Such emitter/detector devices may prove to be very useful in systems employing waveguide transmission lines because they greatly simplify coupling problems, as compared to those encountered when using separate emitters and detectors.

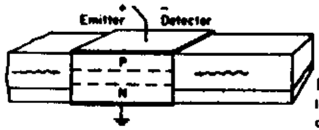

Fig. 15.18. An integrated-optic emitter/detector terminal employing the Franz-Keldysh effect

LINEAR ELECTROOPTIC MODULATORS

REFRACTIVE INDEX CHANGE

$$\Delta n = -n'^3 r' \frac{E}{2}$$

where n' is a linear combination of the principal refractive indices,
r' is a linear sum of the electrooptic coefficients and
E is the appropriate component of the applied electric field

Typical values:

$LiNbO_3$: $\frac{\Delta n}{n} \simeq 0.1\%$

Bulk semiconductor crystals: E.O.-effect: $\frac{\Delta n}{n} \simeq 0.01\%$

Plasma-effects: $\frac{\Delta n}{n} \simeq -1\%$

Quantum Stark-effect
in Multi-Quantum Wells: $\frac{\Delta n}{n} \simeq -1\%$ to a few %

ELECTROOPTIC EFFECTS

- LINEAR E.O. – EFFECT (POCKELS – EFFECT) $\Delta n \sim E$
- QUADRATIC E.O. – EFFECT (KERR – EFFECT) $\Delta n \sim E^2$
- CARRIER INDUCED ABSORPTION AND REFRACTIVE INDEX CHANGES
- FRANZ–KELDYSH EFFECT (SHIFT OF ABSORPTION EDGE TO LONGER WAVELENGTHS AT HIGH ELECTRIC FIELD)
- QUANTUM STARK EFFECT IN MULTI–QUANTUM WELLS

depletion-edge-translation optical waveguide modulators in III-V semiconductors

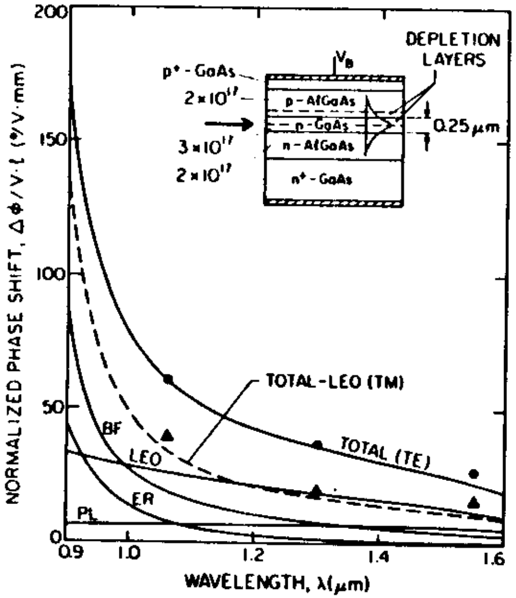

Theoretical and experimental values of normalized phase shift vs wavelength for demonstrated *P/n/N*-AlGaAs/GaAs/AlGaAs configuration. Dots and triangles give measured TE and TM values, respectively. Electric field contributions are: LEO ≡ linear electro-optic and ER ≡ electrorefractive. Carrier contributions are: BF ≡ band filling and PL ≡ plasma.

the higher order electric field (electrorefractive) and carrier (band filling) effects are dominant near the band edge in the depletion-edge-translation (DET) phase modulators

Schrödinger's Equation for the One-Dimensional Motion of a Single Particle

Let us consider a particle of mass m moving along a line, which we may take to be the x-axis, under the action of a force F in the positive x-direction. Also let us suppose that the particle has a potential energy $V(x)$, so that, according to classical mechanics, $F = -dV/dx$.

the state of motion of the particle is in some way represented by a function $\psi(x)$ which satisfies the equation

$$\frac{d^2\psi}{dx^2} + \frac{2m}{\hbar^2}[E - V(x)]\psi = 0. \qquad (1.7)$$

Here $\hbar = h/2\pi$, and E is the constant total energy of the particle, that is, the sum of its kinetic and potential energies. Equation (1.7) is called Schrödinger's Equation, or Schrödinger's *Wave* Equation, for this system, and the function ψ is called a *wave function*.

Particle in a Rectangular Potential Well

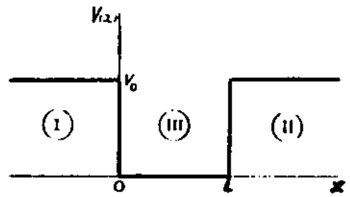

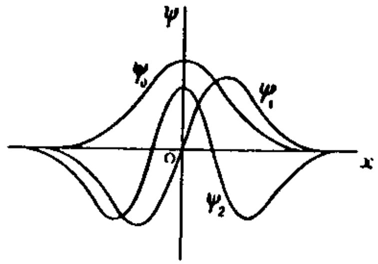

Normalized wave functions for the three states of lowest energy

the allowed energy levels are

$$E_n \approx \frac{h^2\pi^2 n^2}{2mL^2}, \qquad n = 1, 2, 3, \ldots$$

CONFINED-PARTICLE ENERGY LEVELS OF ELECTRONS (short dashed lines), HEAVY (dashed lines) AND LIGHT (long dashed lines) HOLES IN A QUANTUM WELL

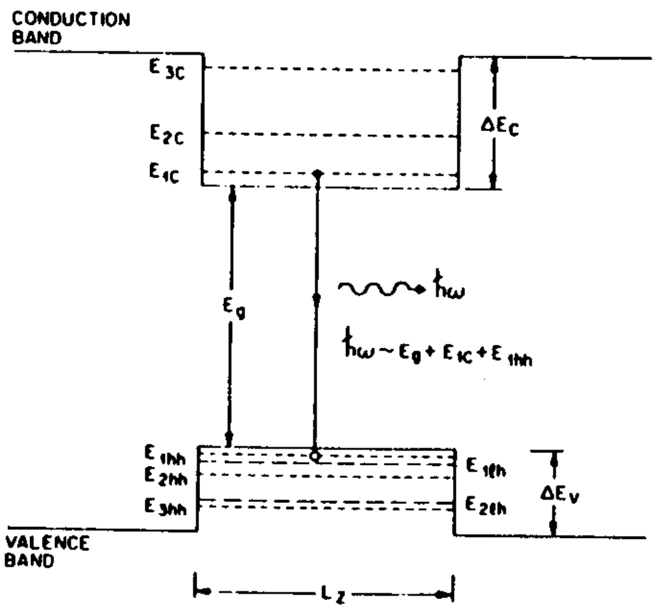

QUANTUM-WELL STRUCTURES

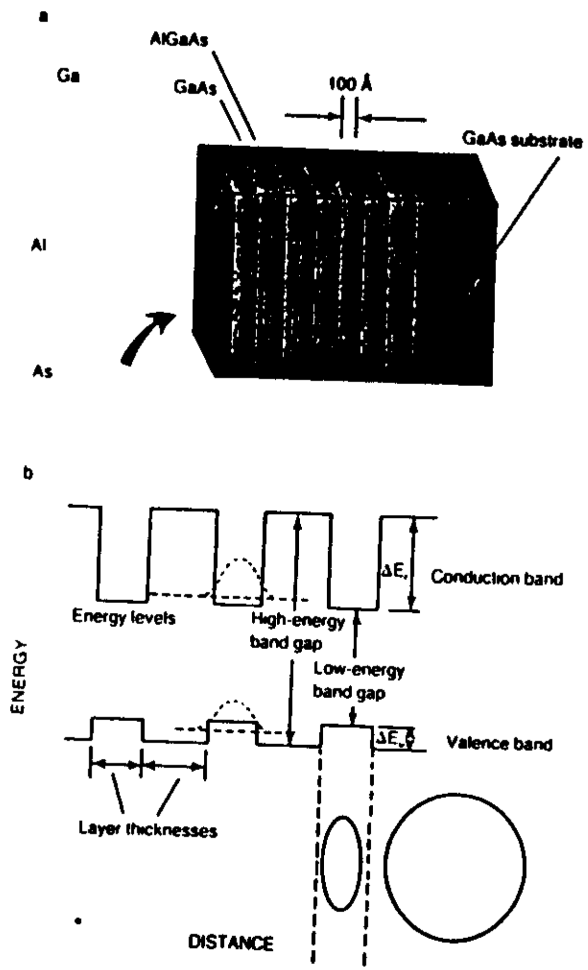

Quantum-well structure and corresponding real-space energy band structure. The schematic diagram in a shows compositional profiling in thin layers. The circle in b represents an exciton in the bulk compound, and the ellipse represents an exciton confined in a layer with a low band gap

33

STARK EFFECT

Frequency shifts of optical spectra of atoms under the influence of electric fields

QUANTUM-WELL STRUCTURES WITH PRONOUNCED EXCITON ABSORPTION PEAKS AT ROOM TEMPERATURE

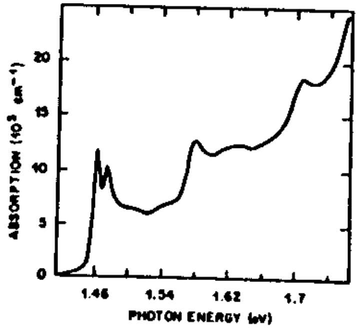

Room temperature absorption spectrum of a GaAs quantum well sample for quantum well thickness ~100Å.

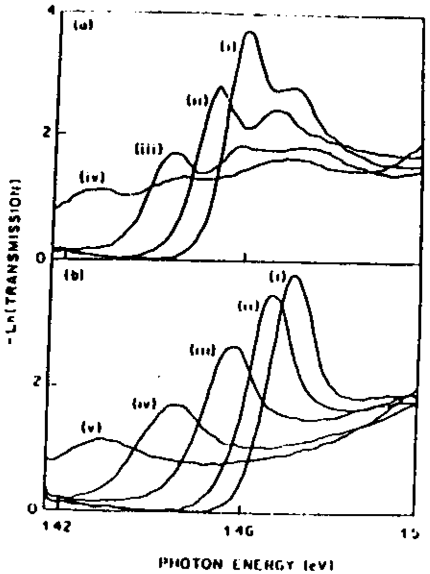

Optical absorption spectra of a GaAs quantum well sample for various fields applied perpendicular to the layers, taken using a waveguide containing two quantum wells: (a) optical electric vector parallel to the layers with fields of (i) 1.6×10^4 V/cm, (ii) 10^5 V/cm, (iii) 1.3×10^5 V/cm, (iv) 1.8×10^5 V/cm; (b) optical electric vector perpendicular to the layers with fields of (i) 1.6×10^4 V/cm, (ii) 10^5 V/cm, (iii) 1.4×10^5 V/cm, (iv) 1.8×10^5 V/cm, (v) 2.2×10^5 V/cm.

QUANTUM CONFINED STARK EFFECT IN MULTI-QUANTUM-WELL STRUCTURES

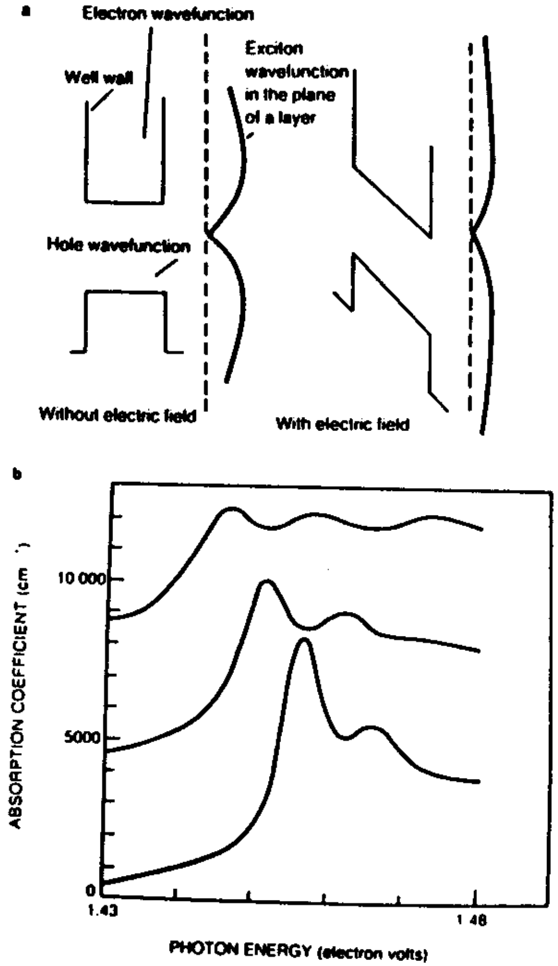

Excitonic wavefunctions without and with an applied electric field (a), and the quantum confined Stark shift in an absorption spectrum (b). The wavefunctions illustrate how the walls of a quantum well hold an electron and hole in a bound state, even at applied fields much stronger than the classical ionization field. The absorption spectra are those of a quantum-well structure under three different static electric fields applied normal to the layers. The fields are 10^4 V/cm (bottom curve), 5×10^4 V/cm (middle curve) and 7.5×10^4 V/cm (top curve)

ELECTRIC FIELD INDUCED REFRACTIVE INDEX VARIATION IN GaInAsP/InP MULTI-QUANTUM WELL STRUCTURES